CO-MAP: Improving Mobile Multiple Access Efficiency With Location Input

Wan Du, *Member, IEEE*, Mo Li, *Member, IEEE*, and Jingsheng Lei

***Abstract*—Based on plenty of sensors on smartphones and tablets, their location information becomes more accurate and easy to access. Many position-based applications have thus been developed. As these mobile devices have become the main access approach of 802.11-based wireless local area networks (WLAN), location information also provides opportunities to improve the performance of underlying wireless communication. This paper presents CO-MAP (Co-Occurrence MAP), which leverages location information to handle exposed and hidden terminal problems, which are still a major cause of throughput degradation in mobile WLANs. With the positions of nodes, CO-MAP rapidly builds a co-occurrence map showing which two links can occur concurrently. Meanwhile, to avoid potential collisions, it selects the best settings of frame transmissions based on a novel analytic network model when hidden terminals are distinguished. CO-MAP improves the goodputs of both downlinks and uplinks in an instant and distributed manner. Our implementation on a hardware testbed demonstrates that CO-MAP can accurately detect potential interferers, and provide significant gain of goodput for both exposed and hidden terminal scenarios. The simulation results also suggest that imperfect position hints can still bring substantial improvement on the multiple access efficiency.**

***Index Terms*—Exposed terminal (ET), hidden terminal (HT), location, mobile wireless network, multiple access.**

I. Introduction

ACCORDING to the statistics of Canalys [2], the total global shipments of smartphones for the whole 2011 overtook client PCs. These "smart" mobile devices have become the main approach to access 802.11-based wireless local area networks (WLAN), which are widely deployed in public entities and private residences. Carrier Sense Multiple Access/Collision Avoidance (CSMA/CA, CSMA for short in this paper) is the basic medium access method for such devices in WLANs. A major problem of CSMA is the performance degradation caused by exposed terminals (ETs) and hidden terminals (HTs) due to the inaccurate estimations of channel condition at receivers by the measurements operated by senders. In two campus WLANs [3], 40% links lose concurrent transmission opportunities due to ETs and 10% links suffer more than 70% throughput reduction because of HTs.

In the 802.11 standards [4], Request-to-Send/Clear-to-Send (RTS/CTS) exchange is an option to mitigate HTs. It is not enabled in many cases due to its overhead and inefficiency of detecting HTs. Moreover, it aggravates the ET problem. Many algorithms achieve a trade-off between preventing HT collisions and increasing spatial reuses by tuning the Carrier Sense (CS) threshold and/or power level [5], [6]. They are highly determined by parameter settings. In recent studies, a common way to enable concurrent transmissions of ETs and avoid HT collisions is to build an interference map of the whole network by site survey and then schedule transmissions accordingly. Like RXIP [7], CMAP [8], and CENTAUR [3], they all learn the interfering relations in WLAN by passive traffic monitoring or online map generation technique [9].

Unlike prior works based on heavy studies of conflicting relations among nodes, the key insight in this work is that, as location information of the current mobile devices has become easily available, we can detect ETs and HTs in WLAN by making proactive use of such information so as to improve the multiple access efficiency. In general 802.11 WLANs, the maximum transmit power of nodes is 100 mW, which provides a communication range of more than 200 m in free space environments and around 50 m for indoor scenarios. On the other hand, based on the plentiful sensor hints on mobile devices, many existing indoor localization approaches [10], [11] offer at least room-level estimation of positions (with an error within 3 m or 5 m). The average outdoor GPS error is 13.7 m in urban outdoor area [12]. Compared to the large communication range of WLAN in indoor and outdoor scenarios, we believe that the accuracy of existing localization techniques provides us considerably meaningful position information to substantially improve the current multiple access design.

By leveraging the location information, this paper presents CO-MAP (Co-Occurrence MAP), which rapidly infers the conflicting relations among nodes. Based on the intrinsic command frame transmissions, location information can be easily shared across all nearby participating nodes with little overhead since large mobility is rare for users in indoor WLAN [13]. With

Manuscript received October 24, 2013; revised January 3, 2014 and March 4, 2014; accepted March 22, 2014. Date of publication April 10, 2014; date of current version December 8, 2014. This work was supported by the Singapore National Research Foundation through its Environmental and Water Technologies Strategic Research Programme, which is administered by the Environment and Water Industry Programme Office (EWI) of the PUB, under Project 1002-IRIS-09; by the NTU Nanyang Assistant Professorship (NAP)under Grant M4080738.020; by the Natural Science Foundation of China under Grants 61272437 and 61373152; by the Innovation Program of Shanghai Municipal Education Commission under Grants 13ZZ131 and 14ZZ150; by the Foundation Key Project of Shanghai Science and Technology Committee under Grant 12JC1404500; and by the Project of Shanghai Science and Technology Committee under Grant 12510500700. A preliminary version of this work was published in Proceedings of IEEE ICDCS 2013 [1]. The associate editor coordinating the review of this paper and approving it for publication was N. Devroye.

W. Du and M. Li are with the School of Computer Engineering, Nanyang Technological University, Singapore 639798 (e-mail: duwan@ntu.edu.sg; limo@ntu.edu.sg).

J. Lei is with the School of Computer and Information Engineering, Shanghai University of Electric Power, Shanghai 200090, China (e-mail: jshlei@shiep.edu.cn).

Color versions of one or more of the figures in this paper are available online at http://ieeexplore.ieee.org.

Digital Object Identifier 10.1109/TWC.2014.2316511

the positions of its relative neighbors within 2-hop, a node computes its conflicting relations with them based on a radio propagation model and a Packet Reception Rate (PRR) model. A co-occurrence map is thus built, by consulting a node which makes the decision on whether or not to enable its transmission concurrently. We propose an enhanced scheduling algorithm to enable most concurrent transmissions when multiple ETs are identified. On the other hand, in order to avoid potential collisions, we select the best settings of frame transmissions for each node based on a novel analytical network model when HTs are distinguished.

Rapid update of interference relations among nodes in CO-MAP is local and lightweight, which is more suitable for mobile WLAN with fast change of network topology. Moreover, based on a distributed design, CO-MAP is able to efficiently schedule the transmissions of both downlinks and uplinks without the concern of central coordinator. In summary, this paper provides three key contributions.

1) *We design CO-MAP, a unified framework that makes proactive use of device positions to handle HT and ET problems in mobile wireless networks*. It improves the network goodput by enabling concurrent transmissions of ETs and mitigating HT collisions.
2) *We implement CO-MAP on commodity hardware platforms*. Experimental results demonstrate that CO-MAP can detect accurately the HTs and ETs, and provide 77.5% gain of goodput for ET scenarios and 34.8% for HT networks.
3) *We also implement CO-MAP on NS-2 to study its performance for large scale networks*. The results show an average increase of 38.5% and 13.5% for the goodput and Jain's fairness index, respectively.

The rest of this paper is organized as follows. Section II reviews related works. Section III introduces the motivation of this work through two benchmarks. Section IV describes the main design of CO-MAP. Some other design details are discussed in Section V. Implementation and evaluation are presented in Section VI. We conclude this paper in Section VII.

II. Related Works

The first work exploring the benefits of integrating sensor hints into wireless network architecture is [14], in which heading and speed hints are used for vehicular network path selection and movement hint is utilized for bit rate adaptation, AP association, and topology maintenance.

HTs and ETs. Giustiniano *et al.* [15] propose a cross-layer estimator at the transceiver side to classify losses caused by noise, collisions of HTs, and unfairness caused by ETs and channel capture. CENTAUR [3] schedules downlink transmissions in centralized enterprise WLAN with a controller based on an online learning technique [9]. However, the time-consuming generation of conflict map (4 s for a topology with ten APs and ten clients) is unsuitable for mobile wireless networks. HTs and ETs are identified by the integration of the information obtained from different APs in [16]. FAST [17] leverages a PHY layer attachment coding to transmit control information and a MAC layer attachment sense to identify HTs and ETs. An out-of-band busy tone and two communication channels (one for control frames and the other for data frames) are used in [18] to handle the HT and ET problems. Nevertheless, these methods all require extra communication channels and are evaluated by simulations.

HTs. Like CO-MAP, the optimal packet size is derived in [19]–[21] to achieve optimal link throughput and/or time-bound fairness of 802.11 Distributed Coordination Function (DCF). However, the HT problem is not considered. DBTMA [22] uses a busy tone sent by receivers to alert their potential HTs. A new MAC is proposed in [23] by combining the mechanism of power control and busy tones to increase channel reuse and reduce co-channel interference with other neighbors. By leveraging the wired Internet network of APs in home WLAN, RXIP [7] schedules the downlink transmissions with token passing.

Several recent works exploit physical layer techniques to recover frames from collisions, such as ZigZag decoding [24] and successive interference cancellation (SIC) [25]. DC-MAC [26] leverages a simultaneous and "free" coordination channel without degrading the effective throughput in the original transmission. They, nevertheless, do not support commodity 802.11 hardware.

ETs. A common way to increase the spatial reuse is multi-channel assignment to potential contending nodes [27], [28]. However, the ET problem in the co-channel is not addressed explicitly in these works. A time division multiplexing approach is proposed in [29] for multi-hop concurrent transmissions in 60 GHz WLAN. CMAP [8] passively monitors the network traffic to build a conflict map with potentially interfering links. The rapid updated co-occurrence map of CO-MAP is more suitable to mobile wireless networks. TRACK [30] harnesses ETs with a rate adaptation approach in enterprise WLANs. Hur *et al.* [31] use location information to verify the mutual impact of two concurrent transmissions. To synchronize ACKs of two concurrent transmissions, the payload of ETs is very limited. CO-MAP overcomes that limitation with the proposed enhanced scheduling algorithm.

III. Motivation

We study the ET and HT phenomena through two experiments using the DCF MAC protocol of 802.11g [4]. To mimic the real deployment of APs in our office, two laptops are deployed with 36 m distance as APs, each of which is associated with a laptop as client. The transmit power of four nodes is set to 0 dBm to shrink the network testbed in one large room. The detailed experiment setting will be described in Section VI.

ETs. To validate the correlation between ETs and their positions, we move one client to different positions to explore ET problems, while two clients are transmitting Transmission Control Protocol (TCP) traffic to their associated AP respectively. Since we want to measure the link bandwidth, we use the saturated traffic load. Fig. 1(a) shows that ETs exist in a large region and they are highly related to their positions. Initially, the client C2 is located 18 m away from AP1, in the middle of two APs. C1 can detect the signal of C2 using CS, and thus, it defers its transmissions while C2 is transmitting. Although the

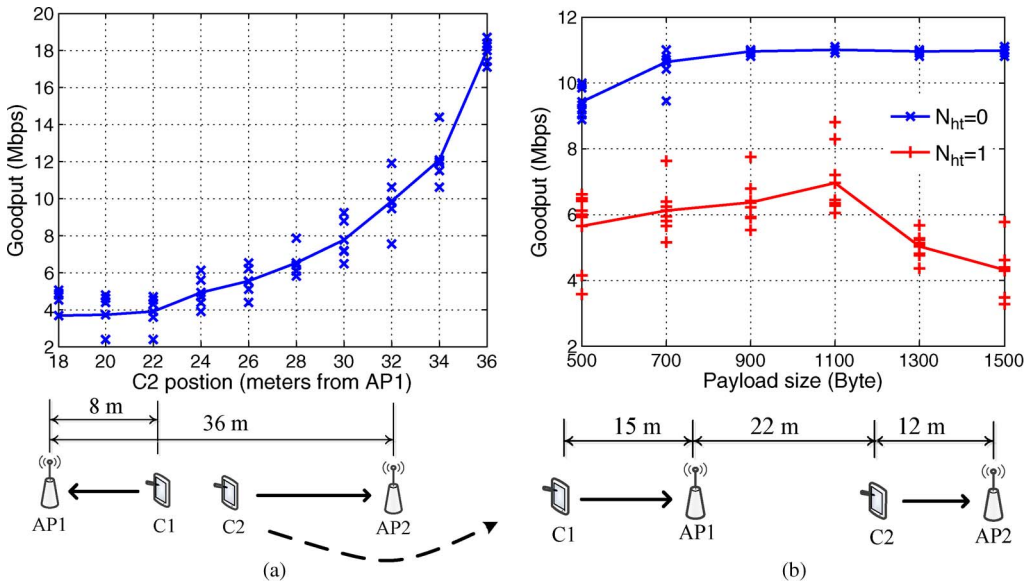

Fig. 1. Goodput of the link from C1 to AP1 and network configuration in exposed terminal scenario (a) and hidden terminal scenario (b).

signal-to-noise ratio at APs are able to support the concurrent transmissions of both clients, they cannot transmit at the same time until C2 moves outside the CS range of C1. The goodput of C1 is increased while C2 is moving away, as the data rate is augmented by the rate adaptation algorithm Minstrel [32]. In Fig. 1(a), when C2 is located 20∼34 m away from AP1, it acts as a potential ET for the link from C1 to AP1. If we could infer this ET scenario through location information of each node, the goodput of the links from C1 to AP1 and from C2 to AP2 can both be improved significantly by enabling the concurrent transmissions with C2's link.

HTs. In the HT experiment, we deploy two clients with a distance of 37 m to create a network under HT interferences, as illustrated in Fig. 1(b). Since C2 cannot sense the signal from C1, they transmit independently; however, when arriving at AP1, C2's signal corrupts the packets from C1. Compared to the ET scenario, the goodput achieved by only one link in this scenario is smaller. The data rate is reduced by the rate adaptation algorithm due to the larger distance between the sender and the receiver.

We vary the packet size while only one link is operating. The goodput of the link from C1 to AP1 without HT augments as the payload size increases as the communication becomes more efficient with long packet size. The augmentation trend is slight since the overhead of channel access and frame header is light for a single operating link. However, with the existence of one HT, the goodput of this link varies, and the best goodput is achieved with a moderate packet size but not the largest one. That is because a larger packet size means a higher probability that the packet is corrupted by potential HTs. Even when the traffic load is heavy, due to the backoff mechanism in DCF, there are some intervals that the channel is free. These intervals could be large when multiple retransmissions occur without success. During the short intervals, if the packet size is short, it has more chance to success. Nevertheless, small packet size also increases the overhead of transmission. Therefore, we believe a proper packet size should be set, according to the number of potential HTs, to achieve an optimal balance between collision probability and transmission efficiency.

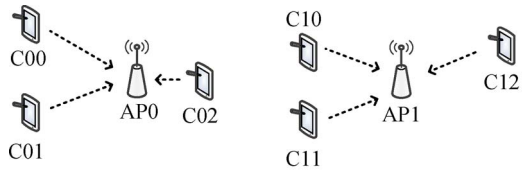

Neighbor table of C11					
Neighbor	C00	C01	C02	C10	C12
X	0	0	40	60	100
Y	0	-20	-10	0	0

Fig. 2. Example of 802.11-based WLAN and neighbor table. X and Y refer to the coordinates of nodes. The location of C00 is the origin of the coordinate plane.

IV. CO-MAP Design

In this section, we present the design of CO-MAP, a unified framework to handle ET and HT problems. A node needs to verify the mutual impact of its transmission and the ongoing one. It should also prevent the potential collisions between multiple ETs. To mitigate collisions of HTs, we select the best parameter setting according to the severity of HT collisions.

A. Preliminary Design of CO-MAP

In CO-MAP, we let each node first report its position to its associated AP, and such position information can be easily shared across all nearby participating nodes. The location exchange can be done with little communication overhead concerning the position upload from clients to APs and download from APs to all other nearby clients. Fig. 2 depicts an example where C11 is able to obtain the positions of other nodes and organize such information into a neighbor table.

Based on the location information, a node estimates its conflicting relations with its neighbors using an accurate radio propagation model (Section IV-B). After that, each node generates a co-occurrence map recording all potential links with which it can transmit concurrently without causing packet loss at both sides. With CO-MAP, on detecting an ongoing transmission, a node verifies its concurrency opportunity by consulting its co-occurrence map. If it succeeds, it competes for channel usage with other ETs using an enhanced scheduling algorithm (Section IV-C). For example, in Fig. 2, C11 can transmit independently to AP1 while C02 is sending packets to AP0; before its transmission, it also needs to assess the channel to avoid collisions with C10, another ET to C02.

With the neighbor table, a node can also find the number of potential HTs by studying the interference relations with its neighbors. By knowing this, it selects the best parameter setting according to an analytical model of networks containing HTs so as to reduce the potential HT collisions and thus increase goodput (Section IV-D). Finally, we analyze the causes of model inaccuracies and their impact to the protocol performance (Section IV-E). Two mechanisms are proposed to recover from the failures of concurrent transmissions.

B. Study of Interference Relations Among Nodes

For a successful transmission in a wireless communication system, a minimum Signal to Interference plus Noise Ratio (SINR) should be guaranteed at the receiver. The minimum SINRs of 802.11b, for example, are normally 10 dB for 11 Mbps down to 4 dB for 1 Mbps. The noise in SINR refers to the noise floor, which includes thermal noise, blackbody, and cosmic noise. It is normally a constant for environments with limited area. A typical noise floor is -95 dBm in 2.4 GHz 802.11 WiFi networks. Therefore, instead of SINR, we use Signal-to-Interference Ratio (SIR) to study the conflicting relations between two links. A node can decode successfully the packets with an SIR larger than a given threshold, T_{SIR}.

To calculate the strength of interference signal, we use the log normal shadowing propagation model, which has been widely applied in many experiments [33]–[35], e.g., wireless interference modeling [33] and deployment of sensor motes [34]. It can accurately capture the radio propagation behaviors for various environments. According to this model, the received signal strength P_d at a given distance d from the transmitter is given by

$$P_d[\text{dBm}] = P_{d_0}[\text{dBm}] - 10\alpha \log\left(\frac{d}{d_0}\right) - X_\sigma \qquad (1)$$

where P_{d_0} represents the received power at a reference distance d_0, α refers to the path loss exponent, and X_σ denotes a zero-mean Gaussian random variable with standard deviation σ drawn from the log normal shadowing distribution. The parameters α and σ can be obtained by the least squares linear regression over measurements conducted across the network area [34].

X_σ models the path loss variation caused by artifacts in the environment. As a result, the received signal strengths at different locations with equal distance to the sender are not the same, and this statistic uncertainty can reflect the impact of shadowing phenomena. While the log normal propagation model captures the signal variations over large scale, the received signal may vary over small distance and time scale due to multipath fading. As in [35], we assume that the overall impact of multipath fading is limited to a few dB. It generally holds true for wideband modulations like 802.11's. Suppose that an interferer is located r meters away from the receiver of an ongoing transmission and the transmit powers of two senders are the same. The packet reception probability of the receiver can be calculated as

$$\begin{aligned} PRR &= Pr\{SIR > T_{SIR}\} \\ &= Pr\left\{X'_\sigma - X_\sigma > T_{SIR} + 10\alpha \log\left(\frac{d}{r}\right)\right\} \\ &= 1 - \Phi\left(\frac{T_{SIR} + 10\alpha \log\left(\frac{d}{r}\right)}{\sqrt{2}\sigma}\right) \end{aligned} \qquad (2)$$

where X_σ and X'_σ are independent values drawn from the log normal shadowing distributions of useful and interfering signals, respectively. The composed variable $(X'_\sigma - X_\sigma)$ is still a zero-mean Gaussian random variable with standard deviation $\sqrt{2}\sigma$. $\Phi(x) = (1/\sqrt{2\pi})\int_{-\infty}^{x} e^{-t^2/2}dt$ is the Cumulative Distribution Function (CDF) of standard normal distribution. A similar model could be found in [36]. The PRR model in (2) is robust to the variation of the parameters α and σ. Assume that the distance between the sender and the receiver (d) is 10 m and T_{SIR} is 10. We can plot the PRR according to different locations of the interferer under different parameter settings, as shown in Fig. 3. The interferer's distance r does not change much for inaccuracy of parameters. For example, the variation caused to the interferer's distance is from 2 m to 7 m if the estimation error of α is 0.5 for PRR of 80%, and it is even smaller for the inaccuracy of σ.

If the addresses of the senders and the receivers are known, based on (2), a node can verify the mutual interferences between any two links. In this work, we mainly focus on scenarios with one interferer. The aggregated impact of multiple HTs and ETs will be handled in future works. However, we will handle the multiple access problem of ETs to avoid the potential collisions among them.

C. ETs

To enable the concurrent transmissions of ETs, in CO-MAP, a node first discovers the ongoing transmission to know the addresses of the sender and receiver and then verifies the feasibility of concurrent transmission to a specific receiver. Before transmission, it executes an enhanced scheduling algorithm to avoid the potential collisions with other ETs. To explore the opportunity of ET transmissions, the MAC addresses of the ongoing transmission should be read by at least one of its ETs.

1) Concurrency Validation: Without RTS/CTS, nodes transmit frame packets directly using CSMA. To enable the discovery of ongoing transmissions, a separate header is encapsulated at the beginning of MAC data. The header includes the destination and source addresses. On receipt of this header, a node recognizes the sender and receiver before

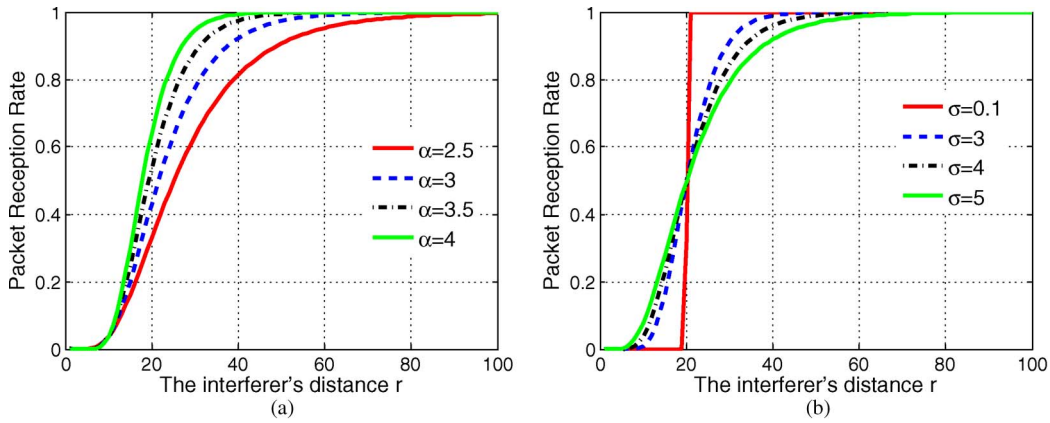

Fig. 3. Impact of α and σ for different locations of the interferer. (a) Path loss α while $\sigma = 4$; (b) Gaussian random deviation σ while $\alpha = 3$.

the incoming frame transmission. This property ensures that nodes start or defer their exposed transmissions in a timely manner.

On detecting an ongoing transmission, a node searches in its neighbor table to find the positions of relative nodes and calculates two distances used in (2), i.e., the distance between the current transmitter and receiver (d) and the distance between itself and the current receiver (r). Based on these distances, the node estimates its interference to the ongoing transmission. If the PRR is larger than a given threshold, T_{PRR}, it infers that its incoming transmission will not interfere with the ongoing transmission.

Meanwhile, to enable a concurrent transmission, the node also needs to verify the impact of the ongoing transmission to its incoming transmission. We also utilize (2), where d now represents the distance between this node and its receiver, and r is the distance between its receiver and the ongoing transmitter. If the result is smaller than T_{PRR}, this node cannot transmit concurrently. It may choose another receiver further away from the current transmitter and verify again; otherwise, it abandons this exposed transmission opportunity and waits for the end of current transmission to compete for channel access with other nodes using CSMA.

In such a way, the position information is converted to the interference relations, which are indicated by PRRs of the node under consideration and one of its neighbors if they transmit simultaneously. The results are recorded in a PRR table, as illustrated in Fig. 4.

2) Co-Occurrence Map: To improve the efficiency, every node builds a co-occurrence map based on the PRR table, as illustrated in Fig. 4. Each entry in this map records one link with which it can transmit concurrently. For a client, it only has one receiver, i.e., its associated AP; therefore, its co-occurrence map only stores possible concurrent links. However, for an AP, an entry of co-occurrence map contains one link and all the potential receivers to which it can transmit concurrently. For example, in Fig. 2, while C02 is sending packets to AP0, C10 can communicate with AP1, and AP1 can transmit to C12 but not C10 and C11.

On detection of an ongoing transmission, the node first searches in its co-occurrence map. If no entry with current link is found, it will verify the concurrency opportunity with this

Neighbor table of C11					
Neighbor	C00	C01	C02	C10	C12
X	0	0	40	60	100
Y	0	-20	-10	0	0

↓

PRR table of C11					
Neighbor	C00	C01	C02	C10	C12
PRR of Neighbor	2.3%	2.3%	97%	0%	0%
PRR of C11	97%	97%	97%	0%	0%

↓

Co-occurrence map of C11	
Source	C02
Destination	AP0

Fig. 4. Location information process of node C11 in the example of Fig. 2: from neighbor table to co-occurrence map with an intermediate transition of packet reception ratio table.

link by computation based on (2). If the validation is passed, this node will start its transmission process immediately. It then inserts this link and its possible concurrent receivers into the co-occurrence map. By doing this, nodes use quick and light-overhead table enquiry to verify concurrency, instead of executing the same calculation repeatedly, when a given transmission occurs. Initially, the co-occurrence map is empty. It is built gradually as the network operates. Therefore, CO-MAP does not require any off-line site survey or suffer from any network performance degradation during initialization.

3) Multiple ETs: An enhanced scheduling algorithm is proposed to avoid collisions among multiple ETs when more than one node succeed in concurrency validation.

For the typical CSMA process in 802.11 DCF, when a node detects an ongoing transmission, it suspends its backoff timer until it finds the medium free for more than DCF Interframe Space (DIFS) duration. After the transmission, it starts a new backoff timer for its next frame transmission, and other nodes resume their frozen backoff process, as illustrated in Fig. 5.

With the enhanced scheduling algorithm of CO-MAP, on receipt of an ongoing transmission, ETs record their current

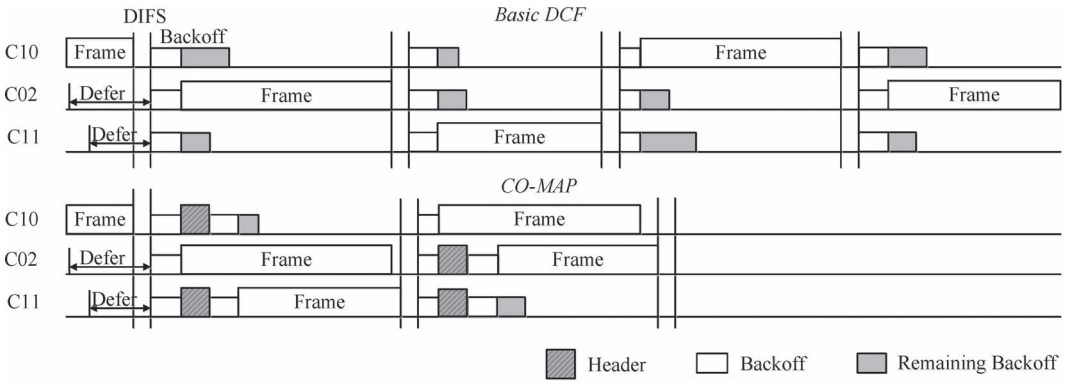

Fig. 5. Communication procedure for basic 802.11 DCF and for the enhanced scheduling algorithm of CO-MAP.

RSSI (named as $RSSI_1$) and resume their backoff process. During the backoff period, they keep monitoring the channel and measuring their RSSI (denoted as $RSSI_2$). If the $RSSI_2$ of an ET holds that $RSSI_2 = RSSI_1 + T'_{cs}$, this node infers that the transmission of another ET occurs and it abandons its concurrent transmission opportunity; otherwise, it starts transmitting when its backoff counter reaches zero. T_{cs} represents the Clear Channel Assessment (CCA) threshold, and T'_{cs} is the part of T_{cs} not containing the noise floor.

One frame includes the transmissions of header, data frame and ACK, one DIFS, and one short interframe space (SIFS). In Fig. 5, while C02 is transmitting, C10 and C11 detect this ongoing transmission by receiving its header. They thus resume their backoff counter. After a short moment, the counter of C11 first expires and it starts transmitting. C10 senses this second transmission and freezes its backoff counter until the transmissions of C02 and C11 finish.

CO-MAP improves the network goodput by enabling extra exposed transmissions. From Fig. 5, we see that CO-MAP provides an almost twofold raise of goodput in this example. Meanwhile, the concurrent transmissions do not cause extra collisions, since ETs still use CS to monitor the channel during the backoff process. The transmission of the final succeeded ET will not interfere with other ongoing transmissions, except the HT problem which exists in the basic 802.11 DCF and will be addressed in Section IV-D. Additionally, CO-MAP increases the network efficiency by parallel transmissions without changing the transmission sequence fixed by the basic 802.11 DCF or adding more extra transmission loads to some particular nodes. It does not thus impact the fairness of basic 802.11 DCF or cause the energy unfairness problem in duty cycle wireless networks, as presented in [37].

4) ACK Loss Problem: Because the ongoing transmission may not finish synchronously with the exposed transmission, their ACKs have a high probability to be corrupted with the remaining data packet transmission. To solve this ACK loss problem, we adopt the selective repeat Automatic Repeat-Request (ARQ) method [38]. This windowed ACK mechanism avoids unnecessary retransmissions of frame packets, in cases that frame packets have been correctly received by receivers but ACKs were lost due to the interferences from ETs.

With selective repeat ARQ, a sender transmits a set of frames with consecutive sequence numbers specified by a window size up to W_{send}. After sending a packet, if no ACK arrives in a short ACK waiting duration, it transmits the next frame in the sending window, instead of retransmitting the non-acknowledged packet. On receipt of a frame, the receiver sends back an ACK with the sequence numbers of all previous missing frames in the window. Therefore, even though some ACKs are lost, the sender can still obtain the knowledge on the transmission results of the frames in the same window. After one window, the sender transmits the lost frames with some new packets in the next window. The window size is set to six packets in our experiments to balance the latency and efficiency.

D. HTs

A collision caused by HTs occurs in three cases. First, a given node starts transmitting when one of its HTs is emitting a radio signal. Second, this node starts transmitting exactly simultaneously with one of its HTs. Third, during the transmission of this node, one of its HTs starts transmitting. Therefore, the HT collision probability is determined by the number of potential HTs and the channel occupancy time of the node under consideration and its HTs.

CO-MAP mitigates the collisions caused by HTs with dynamic adaptation of packet size, according to the number of potential HTs, denoted by N_{ht}. When N_{ht} is large, it uses a short packet size to minimize the channel occupancy of each node and thus reduces the collision probability; otherwise, it adopts a long one to pursue higher transmission efficiency.

1) Number of Potential HTs: For a given link from S to R, its HTs are located inside its interference range and outside the CS range of S. To find the number of potential HTs, by (2), S first finds all interference nodes that may cause its PRR below a certain value if any of them transmits concurrently. Among these nodes, it chooses the ones that are out of its CS range by the propagation model (1).

Due to the effects of random shadowing, every neighbor of S has a probability that its received signal from S is less than a certain CS value, T_{cs} in dBm. Based on (1), we obtain this probability

$$Pr\{P_r < T_{cs}\} = \Phi\left(\frac{T_{cs} - P_{d_0} + 10\alpha \log\left(\frac{r}{d_0}\right)}{\sigma}\right) \quad (3)$$

where r is the distance between the sender and its relative neighbor. The relation between $Pr\{P_r < T_{cs}\}$ and r is monotonically increasing. A larger r corresponds to a higher probability that the signal of$S$ cannot be sensed by this neighbor.

Suppose that we find M interference nodes for a link using (2). They form a set A. Among these nodes, each has a probability, $Pr\{P_r < T_{cs}\}$, of not being able to sense the signal of this link. Therefore, we can treat the number of HTs as a random variable, X, where $x \in S$ and $S = \{0, 1, \ldots, M\}$. $Pr\{X = m\}$ is the sum of all probabilities that m nodes randomly selected in set A have a received signal level below T_{cs} and the other $(M - m)$ nodes do not. There are C_M^m combinations of m selected nodes. Each combination produces a set of m HT nodes and $(M - m)$ contending nodes, denoted by B_i and C_i, where $i = \{1, 2, \ldots, C_M^m\}$ and $C_i = A - B_i$. We refer the $Pr\{P_r < T_{cs}\}$ of each node in B_i as Pr_{ij} and the one in C_i as Pr_{ik}, where $j = \{1, 2, \ldots, m\}$ and $k = \{1, 2, \ldots, M - m\}$. The probability that there are m HTs can be expressed as

$$Pr\{X = m\} = \sum_{i=1}^{C_M^m} \left(\prod_{j \in B_i} Pr_{ij} \prod_{k \in C_i} (1 - Pr_{ik}) \right). \quad (4)$$

Therefore, the average number of potential HTs can be calculated as the expected value of random variable X, as follows:

$$\hat{N}_{ht} = E[X] = \sum_{m=0}^{M} m \cdot Pr\{X = m\}. \quad (5)$$

2) System Model: Bianchi [39] provided an analytical model to study the performance of the IEEE 802.11 DCF MAC protocol under the hypothesis of ideal channel (i.e., no HT and capture). Many works have been conducted to extend it to the HT scenario. A comprehensive summary of existing works can be found in [40], which also proposed a novel analytical model. However, to mitigate HT collisions using previous models, nodes need to know the accurate information across the network (number of HTs and ETs for all neighbors). To provide a simple network model that can be easily implemented in a distributed manner, we develop a novel system model based on Bianchi's model. Each node only needs the number of its contending nodes and HTs. The goodput S of a link from node i in the networks with HTs can be calculated as

$$S_i = \frac{E[Payload\ transmitted\ in\ a\ slot\ of\ node\ i]}{E[Slot\ length]} = \frac{P_s^i L^i}{(1 - P_{tr})T + P_{tr}P_s T_s + P_{tr}(1 - P_s)T_c} \quad (6)$$

where P_s^i represents the probability that the transmission of node i succeeds in a randomly selected time slot, and L^i denotes its payload length. Since HTs do not change the slot length viewed from the point of contending nodes, we use the method in [39] to calculate $E[Slot\ length]$, the average length of slot.

For a link from node i with c contending nodes and h hidden nodes, where $h = \hat{N}_{ht}$ and c can be obtained using the same derivation process of $\hat{N}_{ht}$, P_{tr} refers to the probability that there is at least one transmission in the considered slot. That is

$$P_{tr} = 1 - (1 - \tau)^{c+1} \quad (7)$$

where τ is the probability that a node transmits a frame in a randomly chosen slot time and $\tau = 2/(W + 1)$ for networks with constant backoff window size W. P_s is the probability that a transmission without HTs is successful. T is the empty slot length, T_s is the successful packet transmission time, and T_c represents the expected time for a failed packet transmission. That is

$$P_s = (c + 1)\tau(1 - \tau)^c / P_{tr} \quad (8)$$

$$T_s = T_{HDR} + T_{E[l]} + SIFS + T_{ACK} + DIFS$$

$$T_c = T_{HDR} + T_{E[l^*]} + DIFS. \quad (9)$$

HDR refers to the PHY and MAC header, $E[l]$ and $E[l^*]$ are the average packet length of all nodes and the longest packet size involved in a collision, respectively. For small scale networks, we assume all nodes are homogeneously distributed; therefore, $E[l]$ and $E[l^*]$ are the same throughout the network. For large scale networks, a node chooses a packet size from a set L, where $|L| = N$. $E[l]$ is the average value of all elements in L. We assume that each node has an equal probability colliding with packets of different sizes. This assumption holds if the number of nodes is large. When a node sets its packet size to l_j, where $j \in \{1, 2, \ldots, N\}$ and $l_j < l_{j+1}$, its $E[l^*]$ is given by

$$E\left[l_j^*\right] = \frac{j}{N} l_j + \frac{1}{N} \sum_{k=j+1}^{N} l_k. \quad (10)$$

By considering HTs, a node can transmit successful only at the condition that none of its contending nodes starts transmitting at the same time and none of its HTs starts transmitting one packet transmission time before it starts transmitting or during its transmission; therefore, P_s^i can be given as

$$P_s^i = \tau(1 - \tau)^c \left[(1 - \tau)^h\right]^k \quad (11)$$

where $k = (T_s + T_i)/E[Slot\ length]$ is the average number of slots during the transmissions of node i and one of its HTs. $(1 - \tau)^c$ captures the probability that none of its contending nodes starts transmitting at the same time with the node under consideration. Since the contending nodes can sense the signal from each other, as long as they do not start transmitting exactly simultaneously, there will be no collision. However, due to the fact that HTs cannot sense the signal from the node under consideration, we must consider the duration including one transmission before it starts transmitting or during its transmission.

3) Packet Size Adaptation: Based on the above equations, we can find the best parameter setting to achieve the optimal goodput for the networks with HTs. For a link with five contending nodes and different numbers of HT, we plot its goodputs for various sizes of packet and contention window in Fig. 6, which suggests that there is a best setting of CW and packet size to achieve the highest goodput for different numbers of HTs and contending nodes. We also validate the accuracy of this theoretical system model through NS-2 simulations, as presented in Fig. 6. The explanation of simulation configuration and results will be given in Section VI.

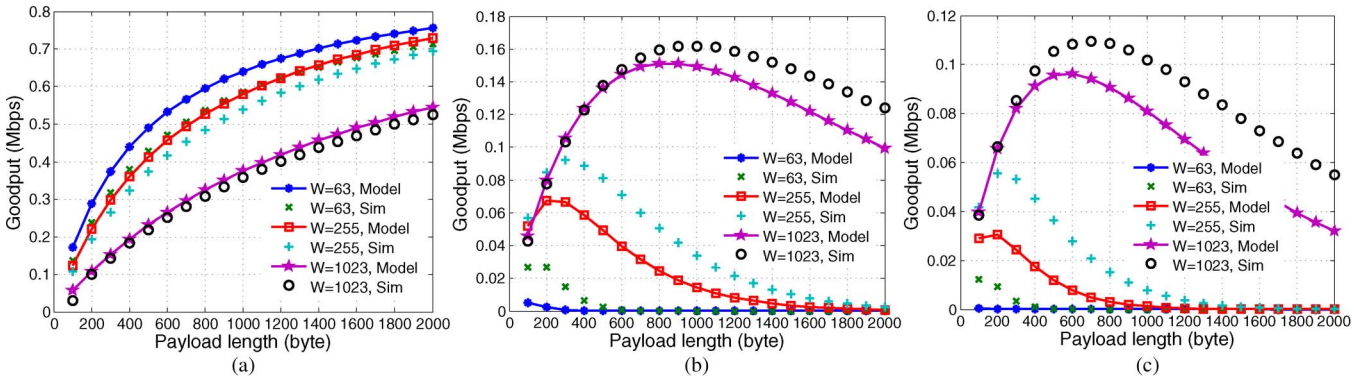

Fig. 6. Theoretical and simulated goodput of a link with several HTs. (a) No HT; (b) three HTs; (c) five HTs.

TABLE I
HIDDEN TERMINAL TABLE OF C00

Number of hidden terminals	2
Number of contending nodes	2

To reduce the computation overhead on mobile devices, we calculate the best packet configurations for different number of HTs and contending nodes beforehand. The results are recorded in a 2-dimension array. An element of the ith row and the jth column represents the best CW and packet size values for a node with i HTs and j contending nodes. The nodes also keep an HT table, which records the number of HTs and contending nodes for each possible receiver it can reach. Therefore, before each transmission, a node with CO-MAP only needs to inquire the HT table and the co-occurrence table. As an example, the HT table of C00 in Fig. 2 is given in Table I. C00 has two HTs (i.e., C10 and C11) and two contending nodes (i.e., C01 and C02).

E. Analysis and Compensation of Inaccuracy

Two main kinds of inaccuracy may impact the performance of CO-MAP. One is the location inaccuracy inherited from GPS data or indoor localization approaches. The other is the log normal shadowing propagation model, which may not be able to exactly capture the dynamic radio channel behaviors. In this section, we analyze the impact of inaccuracy and propose some mechanisms to limit and compensate the performance degradation caused by these inaccuracies.

1) Analysis of Inaccuracy: Both location error and propagation model inaccuracy can cause four categories of misclassification: wrong ET (non-ET nodes inferred as ETs), missing ET (ETs to non-ETs), wrong HT (non-HTs to HTs), and missing HT (HTs to non-HTs). The non-ET nodes can sense and impact the signal of ongoing transmissions, while the ET nodes can sense the signal but do not interfere with the ongoing transmissions. The non-HTs cannot sense or impact the signal from the ongoing transmissions.

Among these four misclassifications, only the wrong ET detection makes the goodput of original system degrade. As a result of this wrong classification, collisions occur if we enable the concurrent transmission of the non-ET nodes. The missing ET detection just causes the miss of concurrent transmission opportunity but does not reduce goodput. The wrong and missing HT detection slightly changes the number of HT which does not impact much our improvement gain of goodput over the basic 802.11 solution. We will show in the evaluation part that the percentage of wrong ET detection is very small (2%) and that CO-MAP can still bring substantial improvement in case of room level location inaccuracy within 10 m.

2) Compensation of Inaccuracy: We propose two mechanisms to limit and handle the failures of concurrent transmission caused by inaccuracies of the location and radio propagation model. First, the co-occurrence map and the neighbor table are flushed periodically to delete the invalid neighbors and update the location information of each node.

Second, the node that enables an exposed concurrent link shall monitor its subsequent transmission results. If it suffers a certain number of transmission failures, it will infer that it is not an ET to this ongoing transmission. It will stop its transmission immediately and modify its co-occurrence map. On the other hand, sometimes, the exposed transmission may succeed, but the ongoing transmission is corrupted. In this case, the ongoing transmitter detects this mistake by a certain number of transmission failures and informs the exposed transmitter to stop the transmission through the AP connection. After that it also updates its co-occurrence map.

V. DISCUSSIONS

Location information exchange. It occurs when a client first joins an AP or its movement is larger a threshold. During the association of a client to an AP, it updates its location information to the AP and downloads the information of neighbors from the AP. One client only needs the information of 2-hop neighbors of its associated AP (neighboring APs of its associated AP and their clients), which is enough to identify HTs and ETs. For instance, in Fig. 2, C10 and C11 are HTs to C00 and C01. Meanwhile, C02 is an ET to C10 and C11. The signals from the clients of other APs far away from the associated AP are too weak to impact the ongoing transmission. The location information can be shared among APs through the wired backbone [7].

The clients also update their location information to AP when their movement is larger than a certain distance, 5 m in our experiment. By doing this, it only causes extra communication overhead when long distance movement happens. Whenever

one client updates its location information, the AP informs its neighboring APs and their clients by broadcasting. User mobility pattern can also be leveraged to adjust the location update process as in [13] and [41].

Implementation of header. In CO-MAP, the header added to normal 802.11 packets to discover ongoing transmissions can be implemented in two ways. One is to insert an extra Frame Check Sequence (FCS) after the sequence number field in MAC PDU, so that the PHY layer can pass the source and destination addresses to upper layers before the receipt of frame payload. This method adds only 4 B overhead on the current 802.11 frame format. However, commodity hardware platforms may not support it. An alternative approach is to send a virtual packet composed of a separated header packet and many data packet, as in [8]. The operation of ET verification involves inquiry of two tables, co-occurrence map and HT table. The computation time of table inquiry by software driver is ignorable compared to the long transmission of this virtual packet. We can also use RTS/CTS to inform all related nodes to the ongoing transmission. The potential ETs can use CTS time to verify whether they can transmit concurrently.

3-D case. In the current version, CO-MAP is mainly designed for 2-D scenario. It can be extended to 3-D environment by updating the coordinate system to 3-D case and considering the height information in calculation. The major difference of 3-D and 2-D is the impact of floor, which is thicker than doors or general walls. This problem can be solved by other specific propagation models, which is left as a future work. Based on the modular design of CO-MAP, when the propagation model is changed, the other components do not need to be modified.

VI. Implementation and Evaluation

We implement CO-MAP on both commodity hardware platforms and NS-2 simulator. In this section, we evaluate the performance of CO-MAP with many experiments on a real testbed and NS-2 simulations.

A. Hardware Testbeds

1) Implementation: In this section, we describe the implementation and setting of experiments for motivation and evaluation. They are performed on the same testbed composed of six laptops with Intel Wireless WiFi Link 4965AGN network adapter running Linux kernel 3.2.0 with MAC80211 and iwlegacy wireless drivers. We implement CO-MAP by extending iwlegacy with three components: (1) generation of co-occurrence map; (2) header and concurrent ET transmission; (3) dynamic packet size adaptation. We use *Iperf*, a widely-distributed network measurement tool. It keeps sending TCP packets from one terminal (or multiple terminals) to another. The throughput of each link is reported every 2 s. For all tests, we disable RTS/CTS due to its limitations, such as overhead, inefficiency, and aggravation of ET problem. The default data rate adaptation algorithm in MAC80211, Minstrel [32], is enabled to verify the effectiveness of CO-MAP under real bit rate conditions.

We mimic the AP layout of our building in campus, where nine APs are deployed on a rectangular floor (25 m $*$ 216 m) of three separated large rooms. Three orthogonal channels in 802.11 are used. The distance between two APs with the same channel is about 69 m. To do the experiment in one laboratory room, the transmit power of APs is set to 0 dBm, and two APs are deployed with a distance of 36 m. By measurements in our office, a large room of 800 m^2 with hard partition panels, α is set to 2.9, and σ is 4 dB for the log normal shadowing propagation model. T_{SIR} is set to 4 for the lowest data rate. The receiving sensitivity is high for the low data rate; therefore, the interfering node could be close to the ongoing receiver. Since we enable the data rate adaptation, when a node infers it is an ET to an ongoing transmission with this low T_{SIR}, it can transmit with a higher data rate if it is located further away from the ongoing transmission. The location of each node are measured manually and thus without any error. We will evaluate the impact of location inaccuracy in Section VI-B.

2) Goodput in ET Scenarios: To verify the goodput improvement provided by CO-MAP over basic DCF, we redo the experiments of Section III with CO-MAP enabled. Results presented in Fig. 7(a) show that CO-MAP can accurately discover the concurrent transmission opportunities and provide 77.5% average increase of goodput. At each position, we measure the throughput for 10 min. Each point on the figure is the average value over 60 samples. We find that C2 plays as an ET for the link from C1 to AP1 when it is located 20$\sim$34 m away from AP1. In this region, we can enable the concurrent transmissions of C1 and C2.

Since the data rate adaptation algorithm is enabled, the goodputs of basic DCF and CO-MAP are both increased as the distance between C2 and AP1 is augmented. When the interferer is located far, its impact to the ongoing transmission is weak and a higher data rate could be used to the link from C1 to AP1 based on a higher signal-to-noise ratio; otherwise, a lower data rate should be adapted. Fig. 7(a) demonstrates that CO-MAP is complementary to the data rate adaptation and can further improve the performance of WLAN under data adaptation. CO-MAP infers a node to be an ET using the lowest data rate corresponding to the shortest distance to the ongoing receiver. If the node is located beyond this distance, a higher data rate can be adapted.

3) Goodput in HT Scenarios: To validate the accuracy of packet size adaptation, instead of one HT in the experiment of Section III, we place three clients around AP2 with various positions to explore different configurations of HT and contending nodes, as illustrated in Fig. 7(b). C2 works as a contending node for the link from C1 to AP1; C3 is a HT; and C4 is an independent node whose transmission has no impact on C1's. We totally configure ten different network topologies by changing the positions of these three clients.

From Fig. 7(b), we see that CO-MAP offers 38.5% mean gain of goodput. When all the clients of AP2 are located far away from AP1, they transmit independently and the goodput of the link from C1 to AP1 achieves the highest value, 11 Mbps. As the number of HTs increases, we reduce the payload size of transmitted packets gradually to maximize the goodput. For instance, when the HT number is 3, we set the payload size to

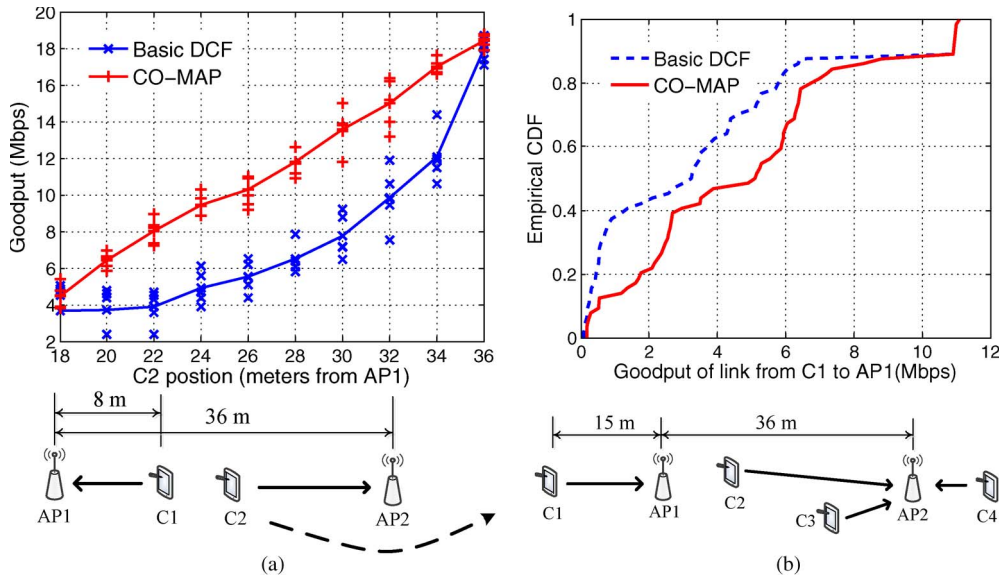

Fig. 7. Goodput of CO-MAP for the link from C1 to AP1 in exposed terminal scenario (a) and hidden terminal scenario (b).

900 B according to the results of the theoretical system model in Section IV-D2.

B. Simulations

With large scale simulations on NS-2, we evaluate the accuracy of the theoretical system model developed in Section IV-D2 and the overall performance of CO-MAP as well as its tolerance to the inaccuracy of position information.

1) Accuracy of the Theoretical System Model: We verify whether (6) can capture the network behaviors with different settings of parameters. The default 802.11 WLAN module distributed in NS-2.35 is used to do this test.

Results presented in Fig. 6 prove that the theoretical system model can accurately capture the network behavior and find the best setting of parameters for networks with different configurations. The highest goodput of a link without HT is achieved with the largest payload length and a small CW size. In this case, because every contending node can detect the transmission of this link using CS, the largest payload length raises the transmission efficiency without causing extra collisions, and a moderate CW size finds a reasonable balance between collision avoidance and transmission efficiency. When the number of HTs increases, CW size should be set to the maximum value to slow down the transmission of all nodes and to reduce their impact on each other; however, a large payload length can still be used to pursue high transmission efficiency. When the number of HTs is large, a small payload length should be used to shorten the channel occupancy time of nodes and thus reduce the collision probability with HTs.

2) Goodput Improvement for Large Scale Networks: In the testbed implementation, because we cannot access the hardware-supported backoff process, on detecting an ongoing transmission, we enable the concurrent transmissions of one ET by disabling its CS with a high CCA threshold. To comprehensively evaluate the performance of CO-MAP, we implement all its functionalities, including the proposed enhanced scheduling algorithm in NS-2.

TABLE II
PARAMETER SETTING FOR THE NS-2 SIMULATIONS

Parameter	Value	Parameter	Value
Data rate	6Mbps	TX power	20dBm
T_{PRR}	95%	T_{cs}	-80dBm
Path loss exponent α	3.3	$T_{cs}^{'}$	-80.14dBm
Standard deviation σ	5dB	T_{sir}	10

We deploy three APs separated about 60 m to mimic the real-life deployment in our office floor. Eight APs with three separate non-overlapping frequency bands are deployed in this floor; only the ones using the same frequency band are considered. Nine clients are randomly deployed around these APs to form 30 distinct topological configurations. By statistics, in this network, 47.6% links have at least one ET and 19.4% links have HTs. All nodes including clients and APs are transmitting Constant Bit Rate (CBR) TCP traffic. The CBR generation rate is set high, 3 Mbps, to emulate the multimedia or VOIP applications, which are commonly used on smartphones. The parameter settings are summarized in Table II. The path loss exponent α and Gaussian random deviation σ of the log normal shadowing propagation model are higher than the testbed experiment, because the network area is larger and the radio environment is more complex. All other parameters are set to the default values of HR/DSSS PHY specifications for the 2.4 GHz band defined in the standard [4]. The results are averaged over 100 simulations.

The CDF of average goodput per link presented in Fig. 8(a) shows that CO-MAP provides 1.385X mean aggregated goodput gain over basic DCF protocol with accurate position information of nodes. In Fig. 8(a), we also display the goodput results in case of 10 m position error range, which will be explained later. Fig. 8(b) demonstrates 13.5% improvement in Jain's fairness index. The improvement of fairness mainly comes from both the concurrent transmission of ETs and the goodput increase of HTs. With fairness improvement simultaneous to goodput gain, these experiments in Fig. 8(a) and

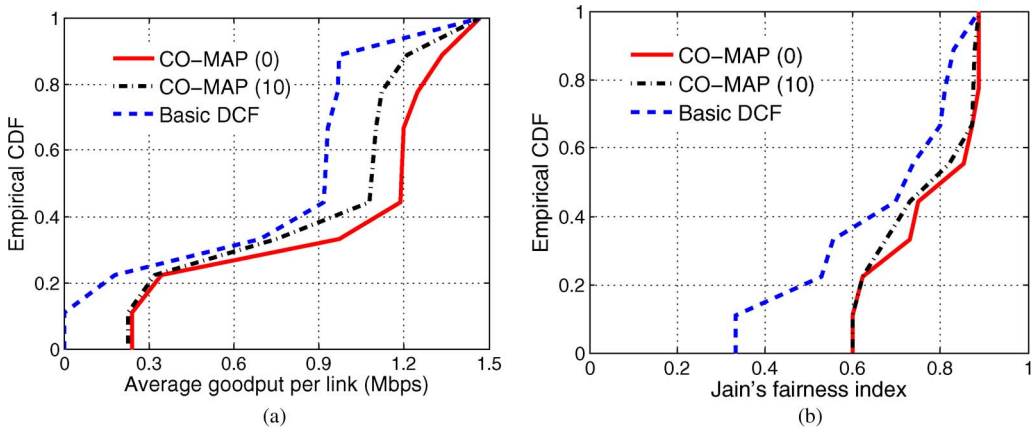

Fig. 8. CDF of goodput (a) and Jain's fairness (b) in large scale network. CO-MAP (0) presents that the perfect position information is used. CO-MAP (10) refers to the cases that a random error within 10 m is added to the position of each node.

TABLE III
MISCLASSIFICATION CAUSED BY LOCATION INACCURACY

Location error range	Wrong ET	Missing ET	Wrong HT	Mising HT
1m	0.2%	0.3%	0.2%	0.2%
5m	1.2%	1.4%	1.1%	0.8%
10m	2.1%	2.3%	2.4%	1.4%

TABLE IV
MISCLASSIFICATION CAUSED BY THE INACCURACY OF THE PARAMETERS (α/σ)

Location error range	Wrong ET	Missing ET	Wrong HT	Mising HT
2.9/5	0.2%	5.4%	0.3%	4.8%
3.3/4	3.6%	0.8%	2.7%	0.7%
3.7/5	7.5%	0.3%	6.7%	0.5%
3.3/6	1.2%	5.3%	0.9%	5.6%

Fig. 8(b) suggest that CO-MAP can efficiently improve the spatial reuse and channel usage with positive scalability of its distributed design.

3) Tolerance to Position Inaccuracy: To verify the tolerance of our approach to the position inaccuracy, we add random error within a certain range to the coordinates of each node in the above experiments. In Fig. 8(a), we see that CO-MAP is still able to provide 18.7% goodput improvement with 10 m position error range. In addition, the improvement of fairness is not impacted by the location error.

To further analyze why CO-MAP can tolerate a large scale of location inaccuracy, we record the wrong detection percentage for different error ranges, as shown in Table III. We record the average percentage of misclassification (introduced in Section IV-E) over 100 simulations. The results in Table III demonstrate that wrong detection of ET and HT in CO-MAP is rare. Even with a maximum error of 10 m that is relatively large for current indoor localization approaches, the misclassification percentage is about 2%. Only the wrong ET detection makes goodput degrade. Its impact is however limited because of its low percentage. The last three misclassifications just limit the improvement of CO-MAP slightly but do not reduce the goodput of original system. We also conduct some simulations for outdoor scenarios with an error range of 30 m for GPS and 100 m communication range; the results are similar with the indoor experiments.

In addition, the parameters (α and σ) in the log normal shadowing propagation model may be inaccurate due to inadequate measurements. To evaluate the sensitivity of CO-MAP to the parameters, we redo the simulations on NS-2 with modified parameter values. The reference setting is 3.3/5. The results of misclassification percentage are presented in Table IV. The misclassification percentage caused by the inaccurate propagation model parameters is small.

VII. CONCLUSION

This paper leverages the room level location information provided by current smartphones and tablets to improve the multiple access efficiency of underlying mobile wireless networks. By converting the position information to a co-occurrence map, it schedules the channel access of multiple ETs in a distributed manner. It also improves the goodput by avoiding collisions according to the number of HTs. With the rapid update of co-occurrence map, CO-MAP enables WLAN to provide users higher performance when they associate with the network without site survey. It is a successful practice of using sensor hints of mobile devices in communication protocol design. The models and techniques developed in this paper can also be applied to the stationary wireless mesh networks where the locations of mesh stations are prior knowledge. We are planning to implement CO-MAP in our mesh sensor network for wind measurement and water quality monitoring [42]. CO-MAP can maximize the exposed concurrent transmissions and mitigate collisions caused by HTs of this network.

REFERENCES

[1] W. Du and M. Li, "Harnessing mobile multiple access efficiency with location input," in *Proc. IEEE ICDCS*, 2013, pp. 246–255.
[2] Smart phones overtake client PCs in 2011, 2012. [Online]. Available: www.canalys.com/newsroom/smart-phones-overtake-client-pcs-2011
[3] V. Shrivastava, N. Ahmed, S. Rayanchu, S. Banerjee, S. Keshav, K. Papagiannaki, and A. Mishra, "CENTAUR: Realizing the full potential of centralized WLANs through a hybrid data path," in *Proc. ACM MobiCom*, 2009, pp. 297–308.
[4] *IEEE Std. 802.11-2007—Part 11: Wireless LAN Medium Access Control (MAC) and Physical Layer (PHY) Specifications*, IEEE Std. 802.11, 2007.
[5] T. S. Kim, H. Lim, and J. C. Hou, "Improving spatial reuse through tuning transmit power, carrier sense threshold, and data rate in multihop wireless networks," in *Proc. ACM MobiCom*, 2006, pp. 366–377.

[6] Y. Liu, L. Ni, and C. Hu, "A generalized probabilistic topology control for wireless sensor networks," *IEEE J. Sel. Areas Commun.*, vol. 30, no. 9, pp. 1780–1788, Oct. 2012.
[7] J. Manweiler, P. Franklin, and R. R. Choudhury, "RxIP: Monitoring the health of home wireless networks," in *Proc. IEEE INFOCOM*, 2012, pp. 558–566.
[8] M. Vutukuru, K. Jamieson, and H. Balakrishnan, "Harnessing exposed terminals in wireless networks," in *Proc. USENIX NSDI*, 2008, pp. 59–72.
[9] N. Ahmed, U. Ismail, S. Keshav, and K. Papagiannaki, "Online estimation of RF interference," in *Proc. ACM CoNEXT*, 2008, pp. 1–12.
[10] K. Wu, J. Xiao, Y. Yi, D. Chen, X. Luo, and L. Ni, "CSI-based indoor localization," *IEEE Trans. Parall. Distrib. Syst.*, vol. 24, no. 7, Jul. 2012.
[11] J. Xiong and K. Jamieson, "ArrayTrack: A fine-grained indoor location system," in *Proc. USENIX NSDI*, 2013, pp. 71–84.
[12] J. Paek, J. Kim, and R. Govindan, "Energy-efficient rate-adaptive GPS-based positioning for smartphones," in *Proc. ACM Mobisys*, 2010, pp. 299–314.
[13] M. Balazinska and P. Castro, "Characterizing mobility and network usage in a corporate wireless local-area network," in *Proc. ACM MobiSys*, 2003, pp. 303–316.
[14] L. Ravindranath, C. Newport, H. Balakrishnan, and S. Madden, "Improving wireless network performance using sensor hints," in *Proc. USENIX NSDI*, 2011, p. 21.
[15] D. Giustiniano, D. Malone, D. J. Leith, and K. Papagiannaki, "Measuring transmission opportunities in 802.11 links," *IEEE/ACM Trans. Netw.*, vol. 18, no. 5, pp. 1516–1529, Oct. 2010.
[16] K. Nishide, H. Kubo, R. Shinkuma, and T. Takahashi, "Detecting hidden and exposed terminal problems in densely deployed wireless networks," *IEEE Trans. Wireless Commun.*, vol. 11, no. 11, pp. 3841–3849, Nov. 2012.
[17] L. Wang, K. Wu, and M. Hamdi, "Combating hidden and exposed terminal problems in wireless networks," *IEEE Trans. Wireless Commun.*, vol. 11, no. 11, pp. 4204–4213, Nov. 2012.
[18] H. Zhai, J. Wang, and Y. Fang, "DUCHA: A new dual-channel MAC protocol for multihop *ad hoc* networks," *IEEE Trans. Wireless Commun.*, vol. 5, no. 11, pp. 3224–3233, Nov. 2006.
[19] C. Dong, P. Yang, S. K. Das, and G. Chen, "Optimal packet size for network throughput with time-bound fairness in IEEE 802.11 networks," *Ad Hoc Sensor Wireless Netw.*, vol. 12, no. 3/4, pp. 253–273, 2011.
[20] J. Yin, X. Wang, and D. P. Agrawal, "Optimal packet size in error-prone channel for IEEE 802.11 distributed coordination function," in *Proc. IEEE WCNC*, 2004, pp. 1654–1659.
[21] M. N. Krishnan, E. Haghani, and A. Zakhor, "Packet length adaptation in WLANs with hidden nodes and time-varying channels," in *Proc. IEEE GLOBECOM*, 2011, pp. 1–6.
[22] Z. J. Haas and J. Deng, "Dual Busy Tone Multiple Access (DBTMA)—A multiple access control scheme for ad hoc networks," *IEEE Trans. Commun.*, vol. 50, no. 6, pp. 975–985, Jun. 2002.
[23] S. L. Wu, Y. C. Tseng, and J. P. Sheu, "Intelligent medium access for mobile ad hoc networks with busy tones and power control," *IEEE J. Sel. Areas Commun.*, vol. 18, no. 9, pp. 1647–1657, Sep. 2000.
[24] S. Gollakota and D. Katabi, "ZigZag decoding: Combating hidden terminals in wireless networks," in *Proc. ACM SIGCOMM*, 2008, pp. 159–170.
[25] S. Gollakota, S. D. Perli, and D. Katabi, "Interference alignment and cancellation," in *Proc. ACM SIGCOMM*, 2009, pp. 159–170.
[26] K. Wu, H. Tan, Y. Liu, J. Zhang, Q. Zhang, and L. M. Ni, "Side channel: Bits over interference," *IEEE Trans. Mobile Computing*, vol. 11, no. 8, pp. 1317–1330, Aug. 2012.
[27] Y. Wu, J. A. Stankovic, T. He, J. Lu, and S. Lin, "Realistic and efficient multi-channel communications in wireless sensor networks," in *Proc. IEEE INFOCOM*, 2008, pp. 1867–1875.
[28] Q. Yu, J. Chen, Y. Fan, X. Shen, and Y. Sun, "Multi-channel assignment in wireless sensor networks: A game theoretic approach," in *Proc. IEEE INFOCOM*, 2010, pp. 1–9.
[29] J. Qiao, L. X. Cai, X. S. Shen, and J. W. Mark, "Enabling multi-hop concurrent transmissions in 60 GHz wireless personal area networks," *IEEE Trans. Wireless Commun.*, vol. 10, no. 11, pp. 3824–3833, Nov. 2011.
[30] J. Huang, G. Xing, and G. Zhou, "Unleashing exposed terminals in enterprise WLANs: A rate adaptation approach," in *Proc. IEEE INFOCOM*, to be published.
[31] S. M. Hur, S. Mao, Y. Hou, K. Nam, and J. Reed, "Exploiting location information for concurrent transmissions in multihop wireless networks," *IEEE Trans. Veh. Technol.*, vol. 58, no. 1, pp. 314–323, Jan. 2009.
[32] Minstrel Description of mac80211. [Online]. Available: linuxwireless.org/en/developers/Documentation/mac80211/RateControl/minstrel/
[33] L. Qiu, Y. Zhang, F. Wang, M. K. Han, and R. Mahajan, "A general model of wireless interference," in *Proc. ACM MobiCom*, 2007, pp. 171–182.
[34] Y. Chen and A. Terzis, "On the implications of the log-normal path loss model: An efficient method to deploy and move sensor motes," in *Proc. ACM SenSys*, 2011, pp. 26–39.
[35] M. Z. Brodsky and R. T. Morris, "In defense of wireless carrier sense," in *Proc. ACM SIGCOMM*, 2009, pp. 147–158.
[36] I. Son, S. Mao, and S. Hur, "Medium access control for opportunistic concurrent transmissions under shadowing channels," *Sensors*, vol. 9, no. 6, pp. 4824–4844, 2009.
[37] Z. Li, M. Li, and Y. Liu, "Towards energy-fairness in asynchronous duty-cycling sensor networks," in *Proc. IEEE INFOCOM*, 2012, pp. 801–809.
[38] A. S. Tanenbaum, *Computer Networks*. Englewood Cliffs, NJ, USA: Prentice-Hall, 2003.
[39] G. Bianchi, "Performance analysis of the IEEE 802.11 distributed coordination function," *IEEE J. Sel. Areas Commun.*, vol. 18, no. 3, pp. 535–547, Mar. 2000.
[40] B. Jang and M. L. Sichitiu, "IEEE 802.11 saturation throughput analysis in the presence of hidden terminals," *IEEE/ACM Trans. Netw.*, vol. 20, no. 2, pp. 557–570, Apr. 2012.
[41] Y. Zhu, L. Ni, and B. Li, "Exploiting mobility patterns for inter-technology handover in mobile networks," *Comput. Commun.*, vol. 36, no. 2, pp. 203–210, Jan. 2013.
[42] C. Liu, Z. Xing, C. H. C. Lloyd, B. He, M. Li, and E. Hans, "Cloud assisted water quality management in Singapore," presented at the Singapore International Water Week, Singapore, 2012.

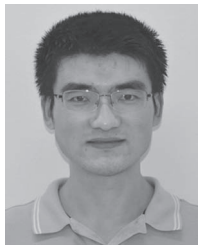

Wan Du (M'13) received the B.E. and M.S. degrees in electrical engineering from Beihang University (formerly known as Beijing University of Aeronautics and Astronautics), Beijing, China, in 2005 and 2008, respectively, and the Ph.D. degree in electrical engineering from the University of Lyon (Ecole Centrale de Lyon), Lyon, France, in 2011.

He is a Research Fellow with the Computer Science Division, School of Computer Engineering, Nanyang Technological University, Singapore. His research interests include wireless and mobile networking, distributed systems, and wireless sensor networks. He is a member of the IEEE.

Mo Li (S'05–M'09) received the B.S. degree in computer science and technology from Tsinghua University, Beijing, China, in 2004 and the Ph.D. degree in computer science and engineering from Hong Kong University of Science and Technology, in 2009. He is a Nanyang Assistant Professor with the Computer Science Division, School of Computer Engineering, Nanyang Technological University, Singapore. His research interests include distributed systems, wireless sensor networks, pervasive computing and RFID, and wireless and mobile systems. He is a member of the IEEE.

Jingsheng Lei is a Professor and the Dean of the College of Computer Science and Technology, Shanghai University of Electronic Power, Shanghai, China. He received the B.S. degree in mathematics from Shanxi Normal University, Linfen, China, in 1987 and the M.S. and Ph.D degrees in computer science from Xinjiang University, Urumqi, China, in 2000 and 2003, respectively.

He has wide research interests, mainly including machine learning, data mining, pattern recognition, and cloud computing. In these areas, he has published more than 100 papers in international journals or conferences. He serves as an Editor-in-Chief of the *Journal of Computational Information Systems*. He is a member of the Artificial Intelligence and Pattern Recognition Technical Committee of the China Computer Federation (CCF), the Machine Learning Technical Committee of the Chinese Association of Artificial Intelligence (CAAI), and the Academic Committee of ACM Shanghai chapter.